PHYSICAL REVIEW E VOLUME 50, NUMBER 4 OCTOBER 1994

Passages and droplets in lamellar fluid membrane phases

Leonardo Golubović
Department of Physics, West Virginia University, Morgantown, West Virginia 26506
(Received 11 July 1994)

We consider thermally excited passages and droplets formed between fluid membranes in a lamellar phase. We show that they induce entropic *attractive* interactions which compete with Helfrich's entropic intermembrane repulsion. This competition determines the intermembrane distance $l_{\max}$ lamellar phases reach at transitions to isotropic fluid membrane phases. In general, $l_{\max}$ is much smaller than the membrane persistence length and crucially depends on membrane saddle-splay ("Gaussian") rigidity.

PACS number(s): 68.15.+e, 05.40.+j, 82.70.Kj

In recent years significant attention has been devoted to statistical physics of fluid membranes [1], and their lamellar and random spongelike phases [2–10]. Membrane fluctuations induce striking effects such as Helfrich's intermembrane repulsion [3] stabilizing lamellar phases [7]. Free energy of this entropic ("steric") repulsion between a pair of membranes at distance l is, per unit membrane area (u.a.),

$$F_{\text{u.a.}}^{\text{steric}} = \text{const} \times \frac{(k_B T)^2}{\kappa l^2}, \tag{1}$$

where κ is membrane bending rigidity [3,4]. Membrane fluctuations are essential also for understanding the lamellar phase melting which occurs when the intermembrane distance l reaches a certain maximal distance $l_{\max}$ [5,8]. de Gennes and Taupin [8] and more recent studies [5,10] identified $l_{\max}$ with fluid membrane *persistence length* ξ_κ [9]. Recent careful experiments, however, appear to contradict this indicating that $l_{\max} \ll \xi_\kappa$ [11].

Prompted by this, here we discuss effects of droplets (vesicles) and passages [as in Fig. 1(a)] thermally excited in a lamellar, L_α phase of surfactant bilayer membranes. We show that their presence induces entropic *attractive* intermembrane interactions which compete with the Helfrich's steric repulsion in Eq. (1) and limit $l_{\max}$. We find that, in general, $l_{\max} \ll \xi_\kappa$. In addition to the persistence length, $\xi_\kappa = a \exp(4\pi\kappa/\alpha k_B T)$ (a is a molecular length scale, and $\alpha = 3$ [9]), we reveal another important scale $\xi_{\bar\kappa} = a \exp(-4\pi\bar\kappa/\alpha' k_B T)$, where $\alpha' = \frac{10}{3}$, and $\bar\kappa$ is the membrane saddle-splay ("Gaussian") rigidity constant [12,13]. We find two distinct lamellar phase behaviors.

(i) Regime A ("Passage regime"). For $0 < -\bar\kappa < (\alpha'/\alpha)\kappa = \frac{10}{9}\kappa$, one has $a \ll \xi_{\bar\kappa} \ll \xi_\kappa$ at low T. In this regime $l_{\max} \sim \xi_{\bar\kappa} \ll \xi_\kappa$. For $l \approx l_{\max}$, there are numerous passages connecting membranes, whereas droplets are rare. Such a lamellar phase melts either into a very dilute droplet phase, or to a sponge phase [if $\|\bar\kappa| - \frac{10}{9}\kappa| < O(1) k_B T$].

(ii) Regime B ("Droplet regime"). For $-\bar\kappa > \frac{10}{9}\kappa$, one has $\xi_{\bar\kappa} \gg \xi_\kappa$ at low T. In this regime $l_{\max} \sim \xi_{\text{drop}} = \xi_\kappa (\xi_\kappa/\xi_{\bar\kappa})^{\alpha'/(2\alpha-\alpha')} \ll \xi_\kappa \ll \xi_{\bar\kappa}$. For $l \approx l_{\max}$ there are numerous droplets between lamellas, whereas passages are rare. Such a lamellar phase melts either into a droplet rich, globular membrane phase or to a sponge phase [if $\|\bar\kappa| - \frac{10}{9}\kappa| < O(1) k_B T$].

Passage regime A apparently corresponds to the experimental situation in egg-lecithin lamellar states studied by Harbich *et al.* [12]. They observe a rise of the density of passages, n_p, with increasing l. We suggest that this rise follows the law $n_p \sim l^{\alpha'-2} = l^{4/3}$, for $l \ll l_{\max}$.

We base our study on the grand-canonical description of fluid membrane ensembles [4,5,10]. Each membrane is characterized by the energy $E = \sigma A + E_{\text{curv}}$, where A is the membrane area, σ is the surface tension ($-\sigma a^2$ is the chemical potential of surfactant molecules), and E_{curv} is the membrane bending energy,

$$E_{\text{curv}} = \int dA \left[\frac{\kappa}{2} H^2 + \bar\kappa G \right], \tag{2}$$

where H and G are, respectively, mean and Gaussian membrane curvature [13]. As in previous studies, we coarse-grain short-scale membrane fluctuations [2,5,10]. This induces a renormalization of the elastic constants in (2) which attain a length scale dependence of the form $\kappa(l) = (\alpha k_B T/4\pi)\ln(\xi_\kappa/L)$, and $\bar\kappa(L) = (\alpha' k_B T/4\pi)\ln(L/\xi_{\bar\kappa})$ [14].

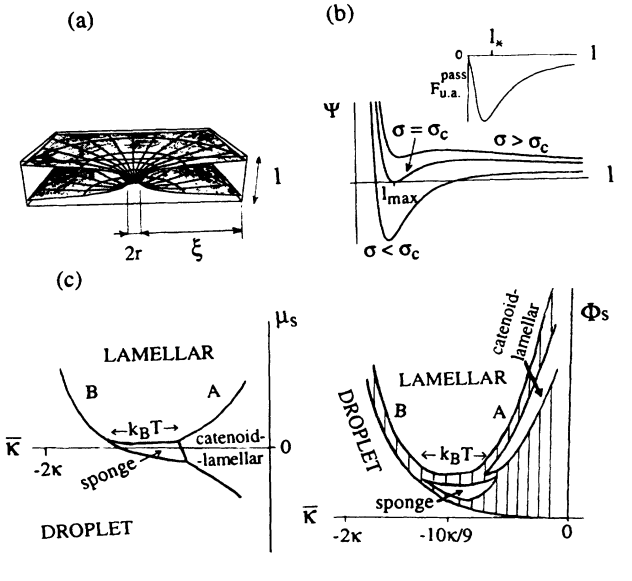

FIG. 1. (a) A passage geometry. (b) $\Psi(l,\sigma)$ for various values of σ. Inset: Passage mediated interaction between lamellas. (c) Schematic phase diagram of fluid membrane systems, for a fixed κ, in the $(\mu_s, \bar\kappa)$ and $(\Phi_s, \bar\kappa)$ planes.

First, we consider a single passage connecting two lamellas at distance l, as depicted in Fig. 1(a). Its curvature energy (2) can be estimated as

$$E_{\rm pass}=O(1)\kappa(\xi)\left(\frac{r}{\xi}\right)^2-4\pi\bar{\kappa}(r), \tag{3}$$

where r is the size of the passage neck, and ξ is the size of the passage deformation region [Fig. 1(a)]. At distances from the neck smaller than ξ, the presence of a passage curves the membranes giving rise to the first term in (3) [15]. The second term in (3) is the Gaussian curvature contribution [12]. The passage deformation region is, approximately, a catenoid [12,15]. This gives the condition $l\approx 2r\ln(\xi/r)$ relating ξ and r in (3). With this constraint, we minimize (3) and find equilibrium passage energy and sizes,

$$E_{\rm pass}=-\alpha' k_BT\ln\left(\frac{l}{\xi_{\bar{\kappa}}}\right), \tag{4}$$

$$\xi_{\rm eq}=O(1)\frac{\left(\frac{\kappa(l)}{k_BT}\right)^{1/2}l}{\ln\frac{\kappa(l)}{k_BT}}, \tag{5a}$$

$$r_{\rm eq}=O(1)\frac{l}{\ln\frac{\kappa(l)}{k_BT}}, \tag{5b}$$

for $K(l)\gg k_BT$, i.e., $l\ll\xi_\kappa$. $E_{\rm pass}$, Eq. (4), is dominated by the Gaussian curvature contribution to Eq. (3). $E_{\rm pass}$ *decreases* with increasing l and, moreover, becomes negative as l crosses $\xi_{\bar{\kappa}}$. By (5a), deformation region size $\xi_{\rm eq}$ *increases* with l.

Next, consider two passages at distance R. They interact via the repulsive potential $U_{pp}(R)\approx\kappa(R)(r_{\rm eq}/R)^2$ [15], for $R<\xi_{\rm eq}$, when the passage deformation regions overlap. By (5), $U_{pp}\approx k_BT$ for $R\approx\xi_{\rm eq}$. For $R>\xi_{\rm eq}$, $U_{pp}<k_BT$, and the passage interaction can be ignored. For $R<\xi_{\rm eq}$, $U_{pp}>k_BT$. Thus the passage interaction can be viewed as a hard core repulsion, with effective hard core size $\approx\xi_{\rm eq}$. Two-dimensional fluid of passages, between a pair of neighboring membranes in a lamellar phase, can be described grand canonically by

$$Z_{\rm pass}=\sum_{N=0}^{\infty}\frac{1}{N!}\prod_{i=1}^{N}\int\frac{d^2\mathbf{X}_i}{\Delta A}\,e^{-H_N/k_BT}, \tag{6}$$

with $\Delta A=l^2[k_BT/\kappa(l)]^2$ [16], and $H_N=NE_{\rm pass}+\Sigma_{i<j}U_{pp}(\mathbf{X}_i-\mathbf{X}_j)$. U_{pp} can be ignored when $|\mathbf{X}_i-\mathbf{X}_j|>\xi_{\rm eq}$, i.e., when the passage number per unit area, n_p, is less than $\xi_{\rm eq}^{-2}$. In this *dilute* regime, (6) yields $n_p(l)\approx n_0(l)$, with

$$n_0(l)=\left(\frac{\kappa(l)}{k_BT}\right)^2\frac{1}{l^2}\left(\frac{l}{\xi_{\bar{\kappa}}}\right)^{\alpha'}\sim l^{\alpha'-2}=l^{4/3}. \tag{7}$$

Free energy of this dilute passage fluid is, per unit membrane area,

$$F_{\rm u.a.}^{\rm pass}(l)=-k_BTn_0(l)\sim -l^{4/3}. \tag{8}$$

By (7), $n_p(l)$ *increases* as $l^{\alpha'-2}=l^{4/3}$. Such a growth of the passage density was indeed observed by Harbich *et al.* in egg-lecithin membrane stacks [12]. By (7) and (8), $n_0\xi_{\rm eq}^2=(l/l_*)^{\alpha'}<1$, with

$$l_*=\left(\frac{k_BT}{\kappa(\xi_{\bar{\kappa}})}\right)^{3/\alpha'}\xi_{\bar{\kappa}}\sim\xi_{\bar{\kappa}}.$$

For $l>l_*$, passage deformations regions overlap and we must take into account passage interactions. As noted above, they are effectively hard core repulsions, with hard core size $\approx\xi_{\rm eq}$. Free energy of the interacting passage fluid can be thus found by minimizing

$$F_{\rm u.a.}^{\rm pass}(n_p,l)=k_BTn_p\ln\frac{n_p}{en_0(l)}-k_BTn_p\ln(1-n_p\xi_{\rm eq}^2), \tag{9}$$

over the passage density n_p. The first term in (9), alone, yields the dilute regime results (7) and (8), whereas the second term is the free energy increase due to excluded volume effects. For dense passage regime, $n_0(l)\xi_{\rm eq}^2=(l/l_*)^{\alpha'}\gg 1$, Eq. (9) yields $n_p\approx 1/\xi_{\rm eq}^2$, i.e., the passage separation $\approx\xi_{\rm eq}$, whereas

$$\begin{aligned}F_{\rm u.a.}^{\rm pass}(l)&\approx -O(1)\frac{k_BT}{\xi_{\rm eq}^2}\ln[n_0(l)\xi_{\rm eq}^2]\\&=-O(1)\frac{\alpha'(k_BT)^2}{\kappa(l)l^2}\ln\frac{l}{l_*}.\end{aligned} \tag{10}$$

$F_{\rm u.a.}^{\rm pass}(l)$ is sketched in the inset to Fig. 1(b). For any l, to a good approximation,

$$\begin{aligned}F_{\rm u.a.}^{\rm pass}(l)&=-O(1)\frac{k_BT}{\xi_{\rm eq}^2}\ln[1+n_0(l)\xi_{\rm eq}^2]\\&=-O(1)\frac{(k_BT)^2}{\kappa(l)l^2}\ln\left[1+\left(\frac{l}{l_*}\right)^{\alpha'}\right],\end{aligned} \tag{11}$$

reducing to (8) for $l\ll l_*$, and to (10) for $l\gg l_*$. The inset to Fig. 1(b) indicates that passages induce an *attractive* interaction between membrane pairs tending to keep membranes at a preferred distance $l=O(1)l_*\sim\xi_{\bar{\kappa}}$. Moreover, by (10) we see that, for $l>l_*$, this passage induced attraction actually *dominates* over Helfrich's steric repulsion (1). Thus total free energy per unit area, $F_{\rm u.a.}^{\rm steric}(l)+F_{\rm u.a.}^{\rm pass}(l)$, also has a minimum at an $l=O(1)l_*\sim\xi_{\bar{\kappa}}$.

In the presence of passages, lamellar phase (l.p.) free energy per unit volume (u.v.) is $F_{\rm u.v.}^{\rm l.p.}(\sigma)=[\Psi(l,\sigma)]_{\min(l)}$ [4], with

$$\Psi(l,\sigma)=\frac{1}{l}[\sigma+F_{\rm u.a.}^{\rm steric}(l)+F_{\rm u.a.}^{\rm pass}(l)]. \tag{12}$$

In the absence of the passage term, $\Psi(l,\sigma)$ has a single minimum for $\sigma<0$, at $l=l_{\rm eq}\sim|\sigma|^{-1/2}$. Thus $l_{\rm eq}$ would diverge as $\sigma\to 0$. By de Gennes and Taupin [8], this infinite swelling of the lamellar phase stops at a melting point where

l_{eq} reaches $l_{max}\sim\xi_\kappa$ and lamellas crumple. Our inclusion of the passage free energy in Eq. (12), however, changes this picture radically for $-\bar\kappa<\frac{10}{9}\kappa$ when $\xi_{\bar\kappa}\ll\xi_\kappa$ (regime A), see Fig. 1(b). l_{eq} minimizing (12) remains finite as $\sigma\to 0$, when $l_{eq}\to O(1)l_*\sim\xi_{\bar\kappa}\ll\xi_\kappa$ and the lamellar phase becomes passage rich. This passage rich lamellar phase remains stable in a range of *positive* values of σ, where a *dilute droplet phase* is typically favored [10]. For $\xi_{\bar\kappa}\ll\xi_\kappa$, free energy of this droplet phase can be shown [by Eq. (19) below] to be zero compared to the energy scale of (12). Thus the lamellar phase transforms into the droplet phase when the minimum of (12) goes to zero. This occurs for a *positive* $\sigma=\sigma_c=+O(1)(k_BT)^2/\kappa(l_*)l_*^2$ [see Fig. 1(b)]. At the transition, l reaches

$$l_{max}=O(1)l_*\sim\xi_{\bar\kappa}\ll\xi_\kappa,$$

for $-\bar\kappa<(\alpha'/\alpha)\kappa=\frac{10}{9}\kappa$ and $\|\bar\kappa|-\frac{10}{9}\kappa|>O(1)k_BT$. Under these conditions (regime A) one thus has a strong first order phase transition between a passage rich, but *still* orientationally well ordered lamellar phase (as $l_{max}\sim\xi_{\bar\kappa}\ll\xi_\kappa$) and a very dilute droplet phase. Prior to this transition, the passage rich smectic-lamellar phase most likely undergoes a weaker transition to a highly anisotropic catenoid-lamellar phase in which passages form regular lattices (with the in-layer lattice constant $\approx\xi_{eq}\approx[\kappa(l)/k_BT]^{1/2}l\gg l$). Such a structural change was indeed observed in egg-lecithin lamellar structures [12].

Let us now consider the lamellar phase behavior in the opposite case with $\xi_\kappa\ll\xi_{\bar\kappa}$, occurring for $-\bar\kappa>\frac{10}{9}\kappa$ and $\|\bar\kappa|-\frac{10}{9}\kappa|>O(1)k_BT$ (regime B). Then, provided $l<\xi_\kappa$, passages will be, by Eq. (7), very dilute. In this regime an important role is played by thermally excited *droplets* (vesicles) confined between lamellas, as discussed hereafter. Curvature free energy (2) of a single nearly spherical droplet of radius R is $E_{drop}(R)=8\pi\kappa(R)+4\pi\bar\kappa(R)=(2\alpha-\alpha')k_BT\ln(\xi_{drop}/R)$, where

$$\xi_{drop}=\xi_\kappa\left(\frac{\xi_\kappa}{\xi_{\bar\kappa}}\right)^{\alpha'/(2\alpha-\alpha')}=a\exp\left[\frac{4\pi(2\kappa+\bar\kappa)}{k_BT(2\alpha-\alpha')}\right] \quad (13)$$

is a new, "droplet" scale. For $2\kappa>-\bar\kappa>\frac{10}{9}\kappa$, one has $a\ll\xi_{drop}\ll\xi_\kappa\ll\xi_{\bar\kappa}$ at low T. Next, consider a polydisperse ensemble of droplets thermally excited between two lamellas at distance l. Its grand-canonical free energy is, in a dilute limit of noninteracting droplets [10],

$$F^{drop}=-k_BT\int dR\,d^2\mathbf{X}\,dz\,\rho_{drop}(R), \quad (14)$$

with

$$\rho_{drop}(R)=\frac{1}{(\Delta R)^4}\exp\left[-\frac{4\pi\sigma R^2+E_{drop}(R)}{k_BT}\right]. \quad (15)$$

$\rho_{drop}(R)dR\,d^2\mathbf{X}\,dz$ is the number of droplets with radii in $(R,R+dR)$ and centers positioned in $d^2\mathbf{X}\,dz$, and $\Delta R=[k_BT/\kappa(R)]^{1/2}R$ (z direction is perpendicular to lamellas). For droplets confined between two lamellas ($2R<l$), Eq. (14) yields, after integrating over z [$\int dz=l-2R$], the droplet free energy, per unit area of a lamella,

$$F^{drop}_{u.a.}(l)=-k_BT\int_a^{l/2}dR(l-2R)\rho_{drop}(R). \quad (16)$$

By (16) and (15), for $|\sigma|l^2/k_BT\ll 1$, one finds

$$F^{drop}_{u.a.}(l)=f^{drop}_{u.a.}(l)+lF^{d.p.}_{u.v.}. \quad (17)$$

Here

$$f^{drop}_{u.a.}(l)=+O(1)\frac{[\kappa(l)]^2}{k_BT}\frac{l^{2\alpha-\alpha'-2}}{\xi_{drop}^{2\alpha-\alpha'}}\sim+l^{2/3}. \quad (18)$$

$f^{drop}_{u.a.}(l)$ is an *attractive* interaction between lamellas. $F^{d.p.}_{u.v.}$ in (17) is the free energy, per unit volume, of the droplet phase,

$$F^{d.p.}_{u.v.}=-O(1)\frac{\kappa^2}{k_BT}\frac{a^{2\alpha-\alpha'-3}}{\xi_{drop}^{2\alpha-\alpha'}}. \quad (19)$$

In the regime B, free energy of the lamellar phase is, per unit volume,

$$F^{l.p.}_{u.v.}=\left(\frac{1}{l}[\sigma+F^{steric}_{u.a.}(l)+F^{drop}_{u.a.}(l)]\right)_{min(l)}.$$

Thus, by (17), we find the *difference* between free energy densities of the lamellar and the droplet phase in the form $F^{l.p.}_{u.v.}-F^{d.p.}_{u.v.}=[\Psi(l,\sigma)]_{min(l)}$, with

$$\Psi(l,\sigma)=\frac{1}{l}[\sigma+F^{steric}_{u.a.}(l)+f^{drop}_{u.a.}]. \quad (20)$$

$f^{drop}_{u.a.}(l)$ here is the droplet mediated interaction, Eq. (18). With changing σ, $\Psi(l,\sigma)$ in (20) behaves (once again) in the manner depicted in Fig. 1(b). For a critical value of σ, $\sigma=\sigma_c=-O(1)(k_BT)^2/\kappa(l_{max})l_{max}^2$, when l reaches its maximal value

$$l_{max}=O(1)\left(\frac{k_BT}{\kappa(\xi_{drop})}\right)^{3/(2\alpha-\alpha')}\xi_{drop}\sim\xi_{drop}, \quad (21)$$

the free energy difference, $[\psi(l,\sigma)]_{min(l)}$, vanishes and the lamellar phase melts into the droplet phase. This droplet phase is actually a globular phase. The largest droplets in this phase are affected by excluded volume effects which limit their size R_{max} [17]. Volume fraction occupied by droplets $\approx\int_a^{R_{max}}(4\pi/3)R^3\rho(R)$ is $O(1)$. This gives

$$R_{max}=O(1)\left(\frac{k_BT}{\kappa(\xi_{drop})}\right)^{2/(2\alpha-\alpha')}\xi_{drop}\sim\xi_{drop}.$$

So, $l_{max}\sim R_{max}\sim\xi_{drop}\ll\xi_\kappa\ll\xi_{\bar\kappa}$, in the regime B with $-\bar\kappa>\frac{10}{9}\kappa$ and $|-\bar\kappa-\frac{10}{9}\kappa|>O(1)k_BT$ [18].

On the other side, for κ and $\bar\kappa$ in the range $|-\bar\kappa-\frac{10}{9}\kappa|<O(1)k_BT$, one has $R_{max}\sim\xi_{drop}\sim\xi_\kappa\sim\xi_{\bar\kappa}$. Thus creation of *passages between the largest droplets* (with $R\approx R_{max}$) is favored in this range. This transforms the globular phase into a sponge phase, which can be envisioned as a condensed liquid phase of droplets connected by passages. A schematic phase diagram summarizing regimes A and B is given in Fig. 1(c). The phase diagram is given for a fixed

$\kappa \gg k_B T$, in the $(\mu_s, \bar{\kappa})$ and (Φ_s, κ) planes. Here $\mu_s = -\sigma a^2$ is the surfactant chemical potential, and Φ_s is the surfactant volume fraction, $\Phi_s = a \partial F_{\text{u.v.}}/\partial \sigma$ [5]. Membrane phases with large structural scales $\gg a$ occur only in a range of *negative* $\bar{\kappa}$, $0 < -\bar{\kappa} < 2\kappa$, consistent with recent careful experiments of Strey [19]. In regime A, one has a coexistence of a very dilute droplet phase (d.p.) with a passage rich catenoid-lamellar phase (l.p.). At their coexistence,

$$\Phi_s^{\text{d.p.}} \approx \frac{a}{l_{\max}} \left(\frac{l_{\max}}{\xi_{\text{drop}}} \right)^{2\alpha - \alpha'} \sim \frac{a}{\xi_{\bar{\kappa}}} \left(\frac{\xi_{\bar{\kappa}}}{\xi_\kappa} \right)^{2\alpha} \ll \Phi_s^{\text{l.p.}} \approx \frac{a}{l_{\max}} \sim \frac{a}{\xi_{\bar{\kappa}}} .$$

On the other side, in regime B, a dense droplet, globular phase coexists with a droplet rich lamellar phase. At their coexistence, $\Phi_s^{\text{d.p.}} \approx a/R_{\max} \sim \Phi_s^{\text{l.p.}} \approx a/l_{\max} \sim a/\xi_{\text{drop}}$ [18].

Finally, let us discuss recent experimental studies of Porte *et al.* [11]. For their ternary system (involving a cosurfactant), $\kappa \approx 3 k_B T$ [thus $\xi_\kappa \approx 300\,000 a$], whereas $\bar{\kappa}$ is not known. By taking tentatively that one is in regime A with $\bar{\kappa} = -\frac{4}{15}\kappa$ (a plausible value in the absence of cosurfactants [20]) for the lamellar phase we get $l_{\max} \sim \xi_{\bar{\kappa}} \approx 100 a$ and $\Phi_s^{\text{l.p.}} \approx a/l_{\max} \sim 1\%$ at the coexistence with the catenoid-lamellar phase. Thus $l_{\max}$ is some three orders of magnitude smaller then ξ_κ, in a striking consistency with the experiments [11]. The experimental $\Phi_s^{\text{l.p.}}$ varies from 5% up to 50% across the phase diagram. This variation is probably due to the cosurfactant (its amount is varied in the phase diagram). Cosurfactants are likely to affect $\bar{\kappa}$, and thus, also, $l_{\max} \sim \xi_{\bar{\kappa}}$. We stress, however, that these experimental data were actually obtained at the coexistence of the lamellar with the sponge phase (rather than the catenoid-lamellar phase). The sponge phase is in Fig. 1(c), present in a range of $\bar{\kappa}$ around $-\frac{10}{9}\kappa$ vanishing as $T \to 0$. At room temperatures, however, this range could be wide enough to explain the stability of the sponge phase of Porte *et al.*

Note added. After completing this research, we learned that Morse independently reached similar conclusions [21].

We thank R. Bruinsma, Z.-G. Wang, R. Strey, and G. Porte for discussions. We acknowledge support of the NSF/WV EPSCoR program.

[1] For a review, see *Statistical Mechanics of Membranes and Surfaces*, edited by D. R. Nelson, T. Piran, and S. Weinberg (World Scientific, Singapore, 1989).

[2] S. A. Safran, D. Roux, M. E. Cates, and D. Andelman, Phys. Rev. Lett. **57**, 491 (1986).

[3] W. Helfrich, Z. Naturforsch. Teil A **33**, 305 (1978).

[4] L. Golubović and T. C. Lubensky, Phys. Rev. B **39**, 12 110 (1989).

[5] L. Golubović and T. C. Lubensky, Phys. Rev. A **41**, 4343 (1990).

[6] D. Roux *et al.*, Europhys. Lett. **11**, 229 (1990).

[7] D. Roux and C. R. Safinya, J. Phys. (Paris) **49**, 307 (1988), and references therein.

[8] P. G. de Gennes and C. Taupin, J. Phys. Chem. **86**, 2294 (1982).

[9] L. Peliti and S. Leibler, Phys. Rev. Lett. **54**, 1690 (1985).

[10] D. A. Huse and S. Leibler, J. Phys. (Paris) **49**, 605 (1988).

[11] G. Porte *et al.*, J. Phys. (Paris) **49**, 511 (1989); G. Porte *et al.*, J. Phys. (France) II **1**, 1101 (1991); M. Skouri *et al.*, *ibid.* **1**, 1121 (1991).

[12] W. Harbich, R. M. Servus, and W. Helfrich, Z. Naturforsch. Teil A **33**, 1013 (1978).

[13] W. Helfrich, Z. Naturforsch. Teil C **28**, 693 (1973).

[14] See, F. David, in Ref. [1], p. 158.

[15] X. Michalet, D. Bensimon, and B. Fourcade, Phys. Rev. Lett. **72**, 168 (1994).

[16] The measure factor in (6) follows from this reasoning: A passage has four collective degrees of freedom: its neck size r [fluctuating around r_{eq}, (5b)], its $\mathbf{X}$ coordinate (parallel to lamellas), and, as the passage can move somewhat also perpendicularly to lamellas ("z direction"), its z coordinate. A general passage partition function includes all passage degrees of freedom, $(r, z, \mathbf{X})$. In the spirit of Huse and Leibler [10], one can use the measure $\int dr/\Delta r \int dz/\Delta r \int\int d^2\mathbf{X}/(\Delta r)^2$, with Δr being the positional uncertainty induced by passage neck thermal roughness $\Delta r \approx r[k_B T/\kappa(r)]^{1/2}$. Fluctuations of z and r can be, however, integrated out of the partition function: $\int dz \approx l$ (since z displacements are limited by lamellas), and $\int dr \approx r_{\text{eq}} \approx l$ [namely, by (3), one can show that $\langle (r - r_{\text{eq}})^2 \rangle^{1/2} \approx r_{\text{eq}}$]. After this, the above measure reduces to that in Eq. (6).

[17] Inclusion of excluded volume effects, however, produces no qualitative changes in Eqs. (17)–(19) [L. Golubović (unpublished)].

[18] Note that, though $l_{\max} \sim R_{\max} \sim \xi_{\text{drop}}$, the length scale $l_{\max}$ is actually smaller than $R_{\max}$ by the factor $[k_B T/\kappa(\xi_{\text{drop}})]^{1/(2\alpha - \alpha')}$ becoming $O(1)$ only at the border between A and B regimes.

[19] R. Strey (unpublished).

[20] Z. G. Wang and S. Safran, J. Chem. Phys. **94**, 679 (1991).

[21] D. Morse, Phys. Rev. E **50**, R2423 (1994).